

Z' searches: prospects for LHC Phase 2

L. Thomas

IIHE ULB-VUB

June 2nd, 2014

1 Introduction: Searches for heavy resonances at the LHC

- Motivations for new physics
- The CMS detector
- Current results
- LHC program for the next 20 years
- Prospects

2 Present work

- Kinematics of dielectron resonances
- Studied properties
- Event selection
- Spin Measurement
- A_{FB} Measurement
- Production modes measurement (gg - $q\bar{q}$ fractions)

3 Conclusions

1 Introduction: Searches for heavy resonances at the LHC

- Motivations for new physics
- The CMS detector
- Current results
- LHC program for the next 20 years
- Prospects

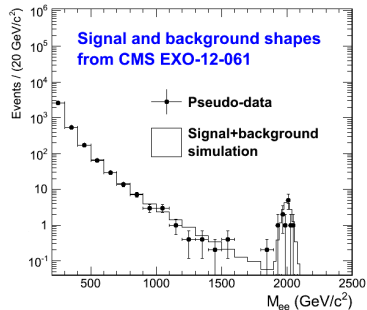
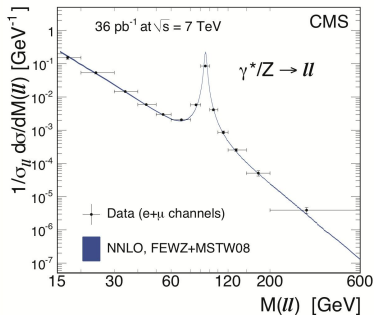
2 Present work

- Kinematics of dielectron resonances
- Studied properties
- Event selection
- Spin Measurement
- A_{FB} Measurement
- Production modes measurement (gg - $q\bar{q}$ fractions)

3 Conclusions

Introduction

- Search for narrow heavy (≥ 1 TeV) resonances decaying into a dielectron pair.
- Generic search also motivated by several theories beyond the Standard Model : Grand Unified Theories (Z'), Large Extra Dimensions (RS gravitons),...
- Main background : Drell-Yan process. Irreducible, interferes with the signal.
- Signature : new peak in the dilepton mass spectrum.

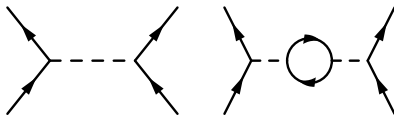


Should we still believe in new physics at the LHC?

- Searches for new physics (i.e. beyond Standard Model) started several decades ago.
- Up to now, despite many efforts, particle colliders didn't find any hint of it...
- The discovery of the scalar boson is an impressive achievement but (so far) doesn't show any deviation from the Standard Model predictions.
- Many BSM theories (e.g. SUSY) are quite tuned:
*"It is very **natural** that we haven't seen it yet but there's a **strong motivation** that it might be discovered soon..."*

All this is quite depressing.

The only source of hope: loop corrections to the scalar boson.



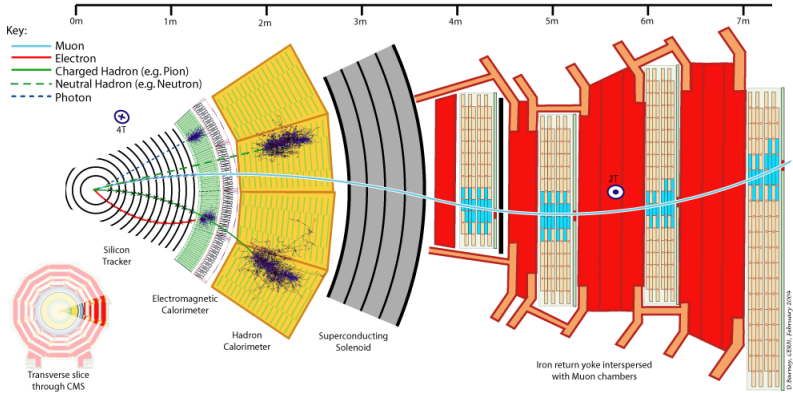
$$\Delta m_H^2 = m_{1-loop}^2 - m_{tree}^2 = -\frac{|\lambda_t|^2}{8\pi^2} \Lambda_{cutoff}^2 + \dots \quad (\text{top quarks})$$

→ **There should really be something at the TeV scale...**

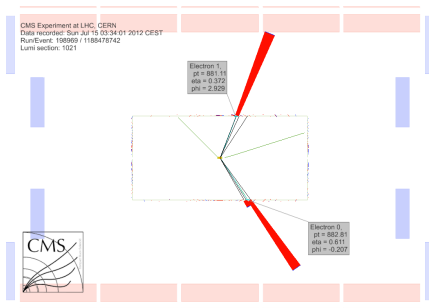
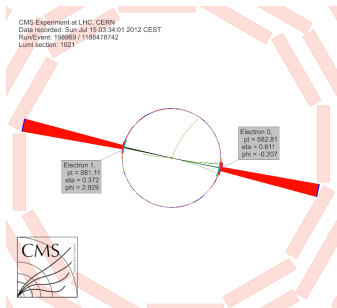
What? Only ~~God~~ Chuck Norris knows...

One of the simplest things to look at: new peak in the dilepton mass spectrum

The CMS detector



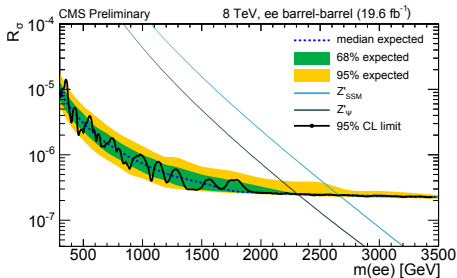
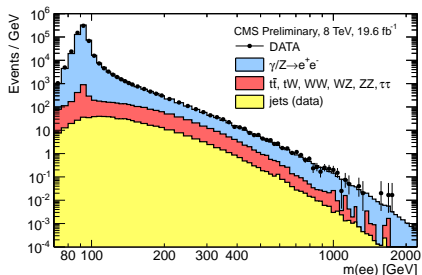
- Selection : 2 isolated high energy electrons.
- Key detectors : tracker, electromagnetic calorimeter.
- Challenge : control electron reconstruction, identification at very high E_T .



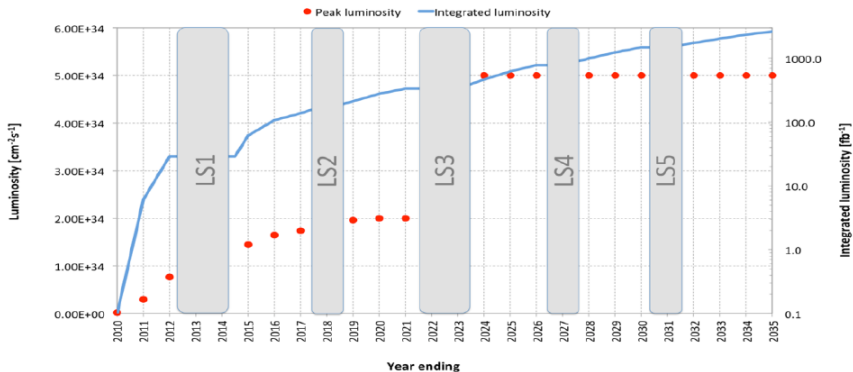
$$M_{ee} = 1776 \text{ GeV}/c^2$$

Latest results presented at Moriond 2013.

- Full 2012 dataset analyzed.
- No signal observed.
- Current limits of Z' ($\sqrt{s} = 8 \text{ TeV}$, 20 fb^{-1}):
 $M \gtrsim 2.7 \text{ TeV}$ for Z'_{SSM} @ 95% CL (ee only)

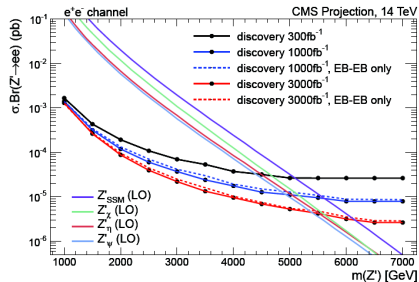


LHC program for the next 20 years



| Name | Period | \sqrt{s} | Peak luminosity | $\int \mathcal{L} dt$ | bunch spacing | Pile up |
|---------|------------|------------|----------------------------------------------------|-----------------------|---------------|---------|
| Run 1 | 2011-2012 | 7-8 TeV | $7.7 \cdot 10^{33} \text{ cm}^{-2} \text{ s}^{-1}$ | 25 fb^{-1} | 50 ns | 20 |
| Phase 0 | 2015-2017 | 13-14 TeV | $1.6 \cdot 10^{33} \text{ cm}^{-2} \text{ s}^{-1}$ | 100 fb^{-1} | 25 ns | 40 |
| Phase 1 | 2019-2021 | 14 TeV | $2 \cdot 10^{33} \text{ cm}^{-2} \text{ s}^{-1}$ | 300 fb^{-1} | 25 ns | 50 |
| Phase 2 | 2023->2030 | 14 TeV | $5 \cdot 10^{33} \text{ cm}^{-2} \text{ s}^{-1}$ | 300 fb^{-1} | 25 ns | 140 |

Projections at 14 TeV:



| | | | |
|-------------------------------|---------------------------------------------------------------------|--------------------------------------------------------------------------|-----------------------------------------------------------------------------|
| Lower limit on $M_{Z'_{SSM}}$ | $\sqrt{s} = 8 \text{ TeV}, 20 \text{ fb}^{-1}$ 2.7 TeV (@95% CL) | $\sqrt{s} = 14 \text{ TeV}, 300 \text{ fb}^{-1}$ 5 TeV (@5 σ) | $\sqrt{s} = 14 \text{ TeV}, 3000 \text{ fb}^{-1}$ 6.2 TeV (@5 σ) |
|-------------------------------|---------------------------------------------------------------------|--------------------------------------------------------------------------|-----------------------------------------------------------------------------|

- For limits settings, \sqrt{s} more important than integrated luminosity.
Cross section of a 4 TeV Z' enhanced by a factor ≈ 100 for $\sqrt{s} = 8 \rightarrow 14 \text{ TeV}$
- Three events is enough to make a discovery.
A discovery in the first months of 2015 is possible !
- In such a case, one wants to characterize the observed signal. \rightarrow More events needed
 \rightarrow **Here comes lumi.**

1 Introduction: Searches for heavy resonances at the LHC

- Motivations for new physics
- The CMS detector
- Current results
- LHC program for the next 20 years
- Prospects

2 Present work

- Kinematics of dielectron resonances
- Studied properties
- Event selection
- Spin Measurement
- A_{FB} Measurement
- Production modes measurement (gg - $q\bar{q}$ fractions)

3 Conclusions

Philosophy of the present study:

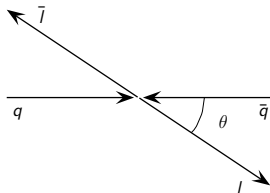
Assume we observe a new resonance at 3-4 TeV in 2015.

- What precision can we reach about its properties?
- Evolution of the uncertainty with lumi? i.e. **Is it worth to collect 3000 fb⁻¹?**
- Use techniques as model independent as possible as the nature of the signal is really unknown.

Practically:

- Take three benchmark models: Z'_ψ , Z'_{SSM} , RS graviton, $M = 3$ and 4 TeV.
- Compare results for 100 fb⁻¹ at $\sqrt{s} = 13$ TeV, and 300/3000 fb⁻¹ at $\sqrt{s} = 14$ TeV.

A 2 body decay provides mainly two observables in addition to the invariant mass:



- $\cos\theta$: angle between the negative lepton and one of the incoming parton (taken to be the quark for $q\bar{q}$ annihilation). Experimentally, approximated by:

$$\cos\theta_{CS_{meas}} = \frac{p_{z,l\bar{l}}}{|p_{z,l\bar{l}}|} 2 \frac{E_l \cdot p_{z,l\bar{l}} - E_{l\bar{l}} \cdot p_{z,l}}{M_{l\bar{l}} \sqrt{M_{l\bar{l}}^2 + P_{T,l\bar{l}}^2}}$$

- $y_{l\bar{l}}$: The dilepton rapidity:

$$y_{l\bar{l}} = \frac{1}{2} \ln \frac{E_{l\bar{l}} + p_{z,l\bar{l}}}{E_{l\bar{l}} - p_{z,l\bar{l}}}$$

Spin determination:

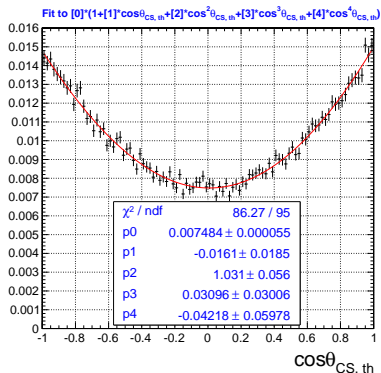
- Spin affects $\cos\theta_{CS}$ through even terms
- Odd terms responsible for A_{FB}
- Different shape for gg and $q\bar{q}$ production modes for spin 2.
- No gg production for a colorless spin 1.

| resonance spin and production mode | $\frac{d\sigma}{d \cos\theta_{CS} }$ |
|-------------------------------------|---------------------------------------------|
| Spin 0 (gg or $q\bar{q}$ fusion) | $\propto 1$ |
| Spin 1 ($q\bar{q}$ fusion) | $\propto 1 + \cos^2\theta$ |
| Spin 2 (gg fusion) | $\propto 1 - \cos^4\theta$ |
| Spin 2 ($q\bar{q}$ fusion) | $\propto 1 - 3\cos^2\theta + 4\cos^4\theta$ |

Spin determination:

- Spin affects $\cos\theta_{CS}$ through even terms
- Odd terms responsible for A_{FB}
- Different shape for gg and $q\bar{q}$ production modes for spin 2.
- No gg production for a colorless spin 1.

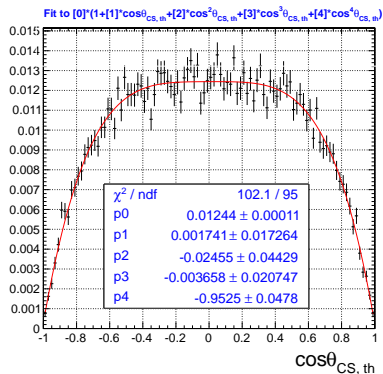
$Z'\psi, M = 3 \text{ TeV}/c^2$



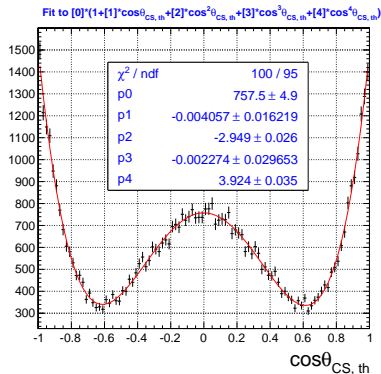
Spin determination:

- Spin affects $\cos\theta_{CS}$ through even terms
- Odd terms responsible for A_{FB}
- Different shape for gg and $q\bar{q}$ production modes for spin 2.
- No gg production for a colorless spin 1.

RS graviton (gg fusion), $M = 3 \text{ TeV}/c^2$



RS graviton ($q\bar{q}$ fusion), $M = 3 \text{ TeV}/c^2$



Forward backward asymmetry measurement A_{FB}

- $A_{FB} = \frac{\sigma_{\theta < \pi/2} - \sigma_{\theta > \pi/2}}{\sigma_{\theta < \pi/2} + \sigma_{\theta > \pi/2}}$
- Affects $\cos\theta_{CS}$ through odd terms.
- No A_{FB} for spin 0.

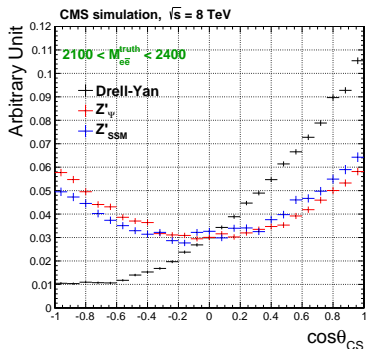
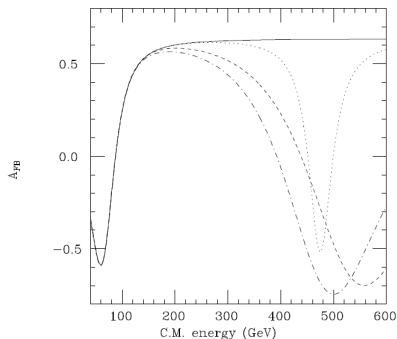


Figure: Left: A_{FB} vs mass for $d\bar{d} \rightarrow e\bar{e}$ for the Standard Model (solid line) and various 500 GeV Z' models (dashed lines). Right: $\cos\theta_{CS}$ for Drell-Yan events and two Z' models.

Production mode fractions

- gg and $q\bar{q}$ production modes possible for a spin 0/2.
- $q\bar{q}$ only for a colorless spin 1.
- Production mode affects the rapidity distribution.

- 2 high energy electrons ($E_T > 35$ GeV)
- For the A_{FB} measurement only: opposite charge requirement (93% efficient for $M=3$ TeV).

$$\text{Acc} \times \text{Eff} = \frac{\text{Selected events with } |M_{reco} - M_{res}|/M_{gen} < 10\%}{\text{Nb of generated events}}$$

| Model, mass | XS (pb) | Acc. \times Eff. | Evs 100 fb ⁻¹ | Evs 100 fb ⁻¹ (Opp. sign) |
|---------------------------|-----------------------|--------------------|--------------------------|--------------------------------------|
| RS Grav (c=0.1), M=3 TeV | 6.1e-04 \pm 1.3e-05 | 0.644 | 39 | 37 |
| RS Grav (c=0.1), M=4 TeV | 5.5e-05 \pm 1.2e-06 | 0.637 | 4 | 3 |
| Z' _{SSM} M=3 TeV | 1.7e-03 \pm 3.5e-05 | 0.495 | 84 | 78 |
| Z' _{SSM} M=4 TeV | 2.6e-04 \pm 4.7e-06 | 0.372 | 10 | 9 |
| Z' _ψ M=3 TeV | 4.5e-04 \pm 1.0e-05 | 0.630 | 28 | 26 |
| Z' _ψ M=4 TeV | 5.1e-05 \pm 1.1e-06 | 0.596 | 3 | 3 |
| DY M>3 TeV | 1.2e-05 \pm 2.2e-07 | 0.666 | 1 | 1 |
| DY M>4 TeV | 1.2e-06 \pm 2.1e-08 | 0.673 | 0 | 0 |

- Low Acc. \times Eff. for Z'_{SSM} because of the cut $|M_{reco} - M_{res}|/M_{res} < 10\%$
- **Background free region.**

Two benchmarks considered here: Z'_ψ , RS graviton ($c=0.1$).

- Same coupling to up and down quarks
- $A_{FB} = 0$ for both

Hypothesis test using a likelihood ratio.

Alternative hypotheses:

- Spin 0 (100% $q\bar{q}$, 50% gg -50% $q\bar{q}$, 100% gg) built by reweighting the $|\cos\theta_{CS,th}|$ distribution of RS gravitons events.
- Spin 1 (100% $q\bar{q}$), using the Z'_ψ distribution
- Spin 2 (100% $q\bar{q}$, 50% gg -50% $q\bar{q}$, 100% gg) built by reweighting the $|\cos\theta_{CS,th}|$ distribution of RS gravitons events.

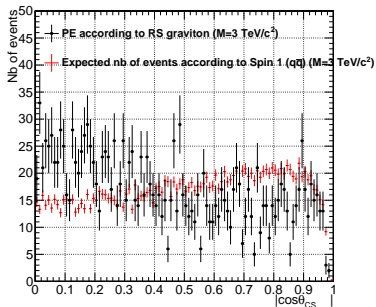
N.B. Distributions used for the pseudo-experiments generation and for the likelihood calculation use disjoint events.

Spin Measurement: Procedure (1)

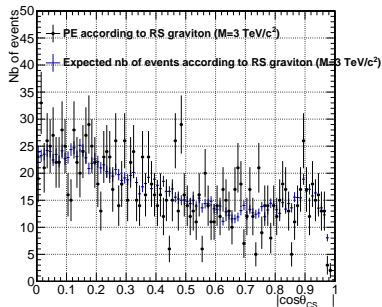
- 1 Generate n events according to H1 (RS graviton or Z' Psi).
- 2 Compute $Q = \ln \frac{\mathcal{L}_0}{\mathcal{L}_1} = \ln \frac{\prod_{i=1}^n p_0(\vec{x}_i)}{\prod_{i=1}^n p_1(\vec{x}_i)}$ where $\vec{x}_i = |\cos\theta_{CS}|$ (1D) or $(|\cos\theta_{CS}|, |y_{ee}|)$ (2D).

1D

CMS simulation $\sqrt{s} = 14$ TeV, 3000 fb $^{-1}$



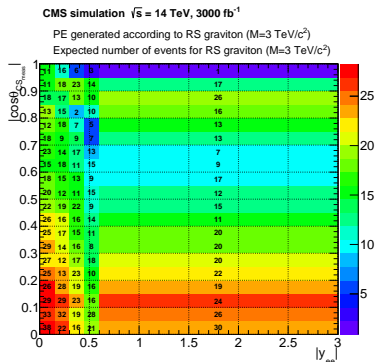
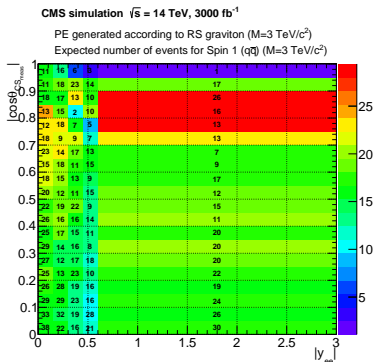
CMS simulation $\sqrt{s} = 14$ TeV, 3000 fb $^{-1}$



Spin Measurement: Procedure (2)

- 1 Generate n events according to H1 (RS graviton or Z' Psi).
- 2 Compute $Q = \ln \frac{\mathcal{L}_0}{\mathcal{L}_1} = \ln \frac{\prod_{i=1}^n p_0(\vec{x}_i)}{\prod_{i=1}^n p_1(\vec{x}_i)}$ where $\vec{x}_i = (|\cos\theta_{CS}|, |y_{ee}|)$ (1D) or $(|\cos\theta_{CS}|, |y_{ee}|)$ (2D).

2D

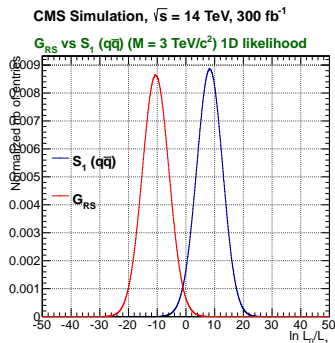


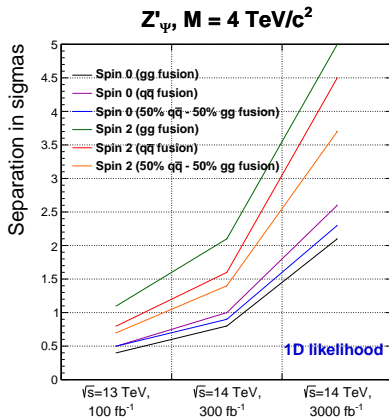
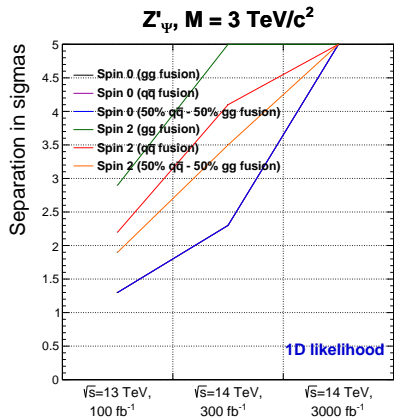
Spin Measurement: Procedure (3)

- 1 Generate n events according to H1 (RS graviton or Z' Psi).
- 2 Compute $Q = \ln \frac{\mathcal{L}_0}{\mathcal{L}_1} = \ln \frac{\prod_{i=1}^n p_0(\vec{x}_i)}{\prod_{i=1}^n p_1(\vec{x}_i)}$ where $\vec{x}_i = |\cos \theta_{CS}|$ (**1D**) or $(|\cos \theta_{CS}|, |y_{ee}|)$ (**2D**).
- 3 Do the same for events generated according to H0 (alternative hypothesis).
- 4 Repeat step 1-3 >1 million times and plot Q for the two scenarios (H0 and H1).
- 5 In the data H1 will be favoured compared to H0 by a confidence level CL_s given by:

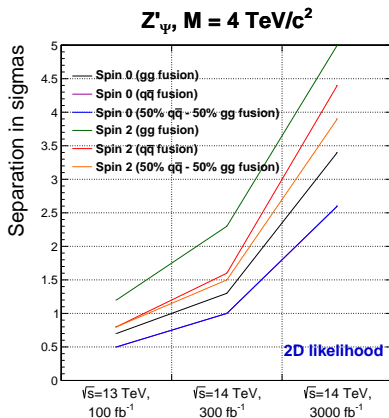
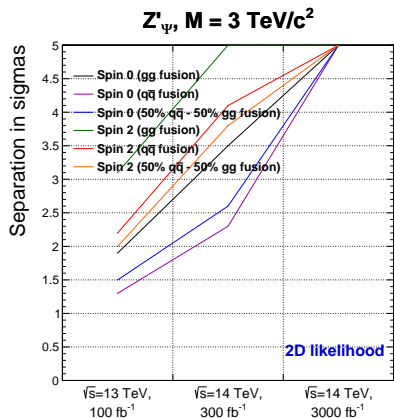
$$CL_s = \frac{\int_{-\infty}^{Q_{obs}} q_1 dQ}{\int_{-\infty}^{Q_{obs}} q_0 dQ}$$

- 6 For projections, take $Q_{obs} = Q_{mean}(H1 \text{ true})$.
- 7 Separation in σ obtained by:
 $\sqrt{2} \text{InverseErf}(1 - CL_s)$





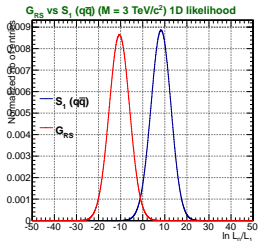
- 3000 fb^{-1} allows one to exclude all wrong spin hypotheses for a $4 \text{ TeV } Z'_\psi$ at $> 2\sigma$.
- 3000 fb^{-1} allows one to exclude all wrong spin hypotheses for a $3 \text{ TeV } Z'_\psi$ at $> 5\sigma$.
Similar results for RS graviton.



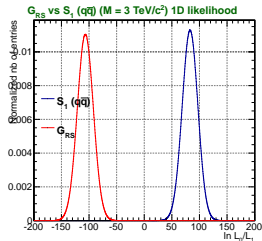
- Slight improvement compared to the 1d method. → Information better used. Similar results for RS graviton.

Spin measurement: Likelihood ratios 1D

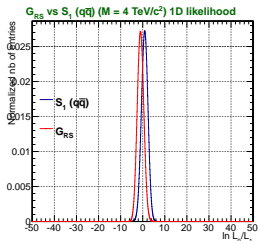
CMS Simulation, $\sqrt{s} = 14$ TeV, 300 fb⁻¹



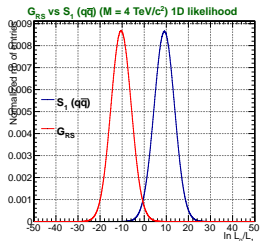
CMS Simulation, $\sqrt{s} = 14$ TeV, 3000 fb⁻¹



CMS Simulation, $\sqrt{s} = 14$ TeV, 300 fb⁻¹

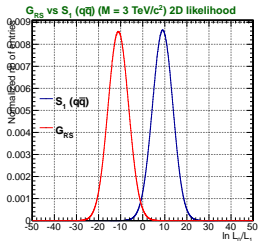


CMS Simulation, $\sqrt{s} = 14$ TeV, 3000 fb⁻¹

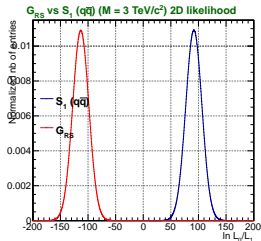


Spin measurement: Likelihood ratios 2D

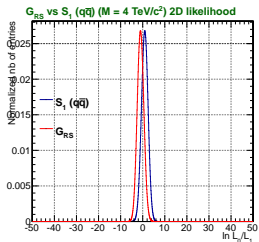
CMS Simulation, $\sqrt{s} = 14$ TeV, 300 fb⁻¹



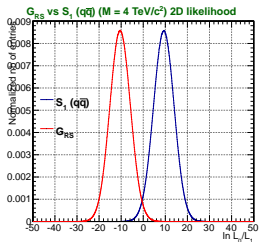
CMS Simulation, $\sqrt{s} = 14$ TeV, 3000 fb⁻¹



CMS Simulation, $\sqrt{s} = 14$ TeV, 300 fb⁻¹

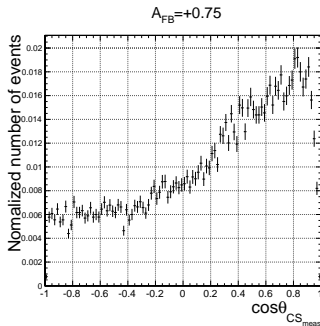
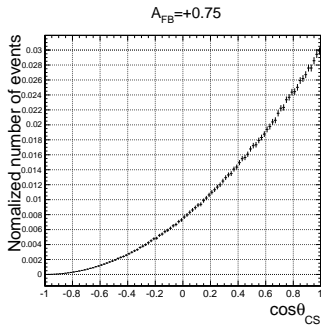


CMS Simulation, $\sqrt{s} = 14$ TeV, 3000 fb⁻¹



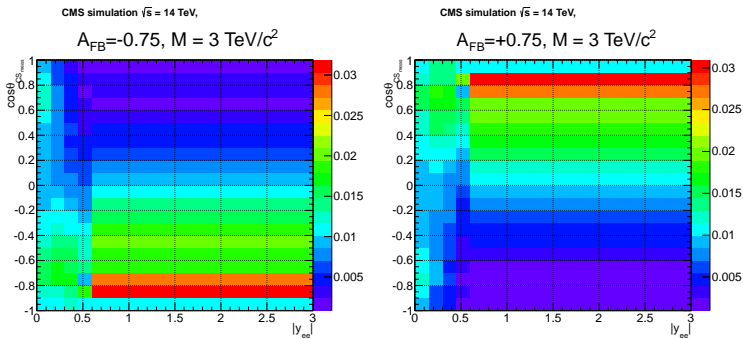
A_{FB} measurement: Generalities (1)

- Only non zero for a spin 1 or 2 resonance. (also 0 for spin 2 gravitons)
- Here focusing on spin 1 particle.
- Needs to distinguish the electron from the positron
- The $\cos\theta$ distribution for a spin 1 is $\propto 1 + \cos^2\theta + \frac{8}{3}A_{FB}\cos\theta$ (with $A_{FB} \in [-0.75, 0.75]$)
- Experimental $\cos\theta_{CS}$ distorted by ambiguity in quark direction determination.



A_{FB} measurement: Generalities (2)

- Only non zero for a spin 1 or 2 resonance. (also 0 for spin 2 gravitons)
- Here focusing on spin 1 particle.
- Needs to distinguish the electron from the positron
- The $\cos\theta$ distribution for a spin 1 is $\propto 1 + \cos^2\theta + \frac{8}{3}A_{FB}\cos\theta$ (with $A_{FB} \in [-0.75, 0.75]$)
- Experimental $\cos\theta_{CS}$ distorted by ambiguity in quark direction determination.
 $\Rightarrow |y_{ee}|$ **can improve the measurement.**



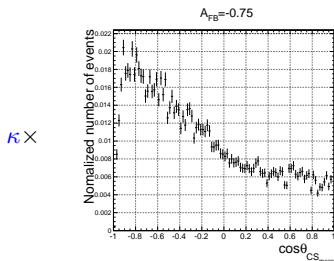
Quark direction better identified at high y_{ee}

A_{FB} measurement: Procedure (1)

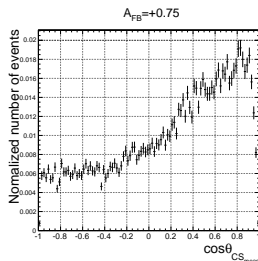
- 1 Generate events according to the studied sample (Z'_ψ or Z'_{SSM})
- 2 Generate the $\cos\theta_{CS}$ distribution for a model with $A_{FB} = \pm 0.75$:
 $p_{A_{FB}=-1}(\cos\theta_{CS_{meas}})$, $p_{A_{FB}=+1}(\cos\theta_{CS_{meas}})$,
- 3 Find κ such that:

$$\kappa * p_{A_{FB}=-1}(\cos\theta_{CS_{meas}}) + (1 - \kappa) * p_{A_{FB}=+1}(\cos\theta_{CS_{meas}})$$

maximizes the likelihood.



$+ (1 - \kappa) \times$



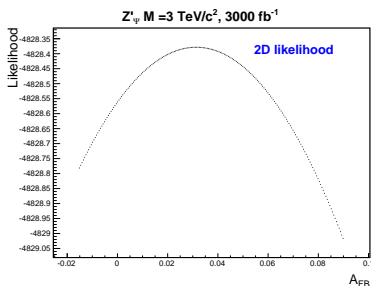
A_{FB} measurement: Procedure (2)

- 1 Generate events according to the studied sample (Z'_ψ or Z'_{SSM})
- 2 Generate the $\cos\theta_{CS}$ distribution for a model with $A_{FB} = \pm 0.75$:
 $p_{A_{FB}=-1}(\cos\theta_{CS_{meas}})$, $p_{A_{FB}=+1}(\cos\theta_{CS_{meas}})$,
- 3 Find κ such that:

$$\kappa * p_{A_{FB}=-1}(\cos\theta_{CS_{meas}}) + (1 - \kappa) * p_{A_{FB}=+1}(\cos\theta_{CS_{meas}})$$

maximizes the likelihood.

- 4 $A_{FB,meas} = \frac{3}{4}(2\kappa - 1)$ ¹



¹see backups

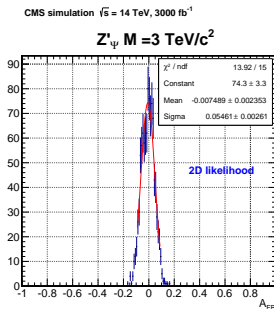
A_{FB} measurement: Procedure (3)

- 1 Generate events according to the studied sample (Z'_ψ or Z'_{SSM})
- 2 Generate the $\cos\theta_{CS}$ distribution for a model with $A_{FB} = \pm 0.75$:
 $p_{A_{FB}=-1}(\cos\theta_{CS_{meas}})$, $p_{A_{FB}=+1}(\cos\theta_{CS_{meas}})$,
- 3 Find κ such that:

$$\kappa * p_{A_{FB}=-1}(\cos\theta_{CS_{meas}}) + (1 - \kappa) * p_{A_{FB}=+1}(\cos\theta_{CS_{meas}})$$

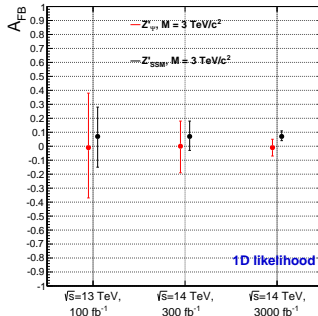
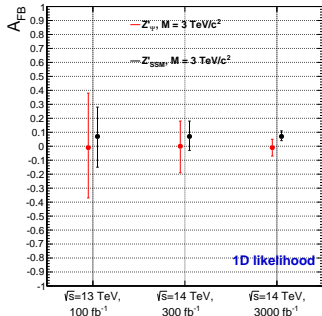
maximizes the likelihood.

- 4 $A_{FB,meas} = \frac{3}{4}(2\kappa - 1)$
- 5 Repeat the procedure 1000 times to find the median and the $\pm 1\sigma$ band.



Same technique is applied for the 2D distributions ($\cos\theta_{CS_{meas}}, |y_{ee}|$).

A_{FB} measurement: Results 1D

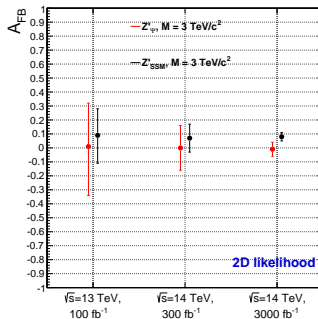
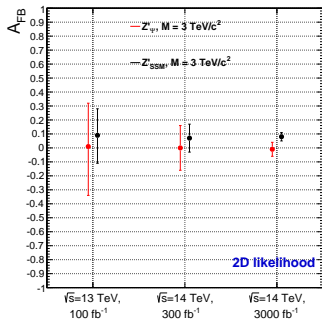


Predicted values:

| | up quarks | down quarks | $\sqrt{s} = 13$ TeV pp collisions |
|-----------------------|-----------|-------------|-----------------------------------|
| Z'_ψ | 0 | 0 | 0 |
| Z'_{SSM} | 0.075 | 0.105 | 0.08 |
| Drell-Yan $M > 3$ TeV | 0.595 | 0.625 | 0.60 |

(Results for $M=4$ TeV in the backups)

A_{FB} measurement: Results 2D



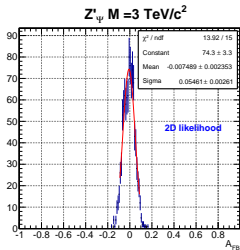
Predicted values:

| | up quarks | down quarks | $\sqrt{s} = 13 \text{ TeV}$ pp collisions |
|-------------------------------|-----------|-------------|-------------------------------------------|
| Z'_{ψ} | 0 | 0 | 0 |
| Z'_{SSM} | 0.075 | 0.105 | 0.08 |
| Drell-Yan $M > 3 \text{ TeV}$ | 0.595 | 0.625 | 0.60 |

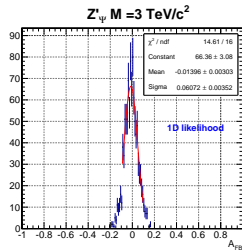
2D method improves precision by $\approx 10\%$.

(Results for $M=4 \text{ TeV}$ in the backups)

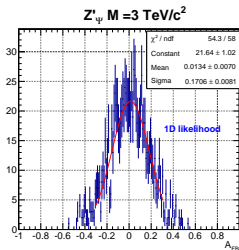
CMS simulation $\sqrt{s} = 14$ TeV, 3000 fb⁻¹



CMS simulation $\sqrt{s} = 14$ TeV, 3000 fb⁻¹



CMS simulation $\sqrt{s} = 14$ TeV, 300 fb⁻¹



- Angular distribution and rapidity distributions affected by production mode for spin 2.
- Only rapidity distributions affected by production mode for spin 0.
- Those fractions are mass dependent (related to the pdfs).
- Here, we focused on the measurement of the RS graviton $qq/q\bar{q}$ fractions for $M = 3, 4 \text{ TeV}/c^2$.
- **Those fractions are also \sqrt{s} dependent. This was neglected in the 13 TeV \rightarrow 14 TeV extrapolation**

Procedure:

- same than for A_{FB} measurement. This time, κ runs from 0 (pure gg fusion) to 1 (pure $q\bar{q}$ fusion)

1D

| | 100 fb ⁻¹ (13 TeV) | 300 fb ⁻¹ (14 TeV) | 3000 fb ⁻¹ (14 TeV) |
|---------------------------------------------|----------------------------------------|----------------------------------------|----------------------------------------|
| R-S graviton (M = 3 TeV/c ²) 1D | 0.35 ^{+0.33} _{-0.32} | 0.36 ^{+0.16} _{-0.15} | 0.36 ^{+0.05} _{-0.05} |
| R-S graviton (M = 4 TeV/c ²) 1D | 0.34 ^{+0.67} _{-0.34} | 0.19 ^{+0.56} _{-0.19} | 0.24 ^{+0.15} _{-0.16} |

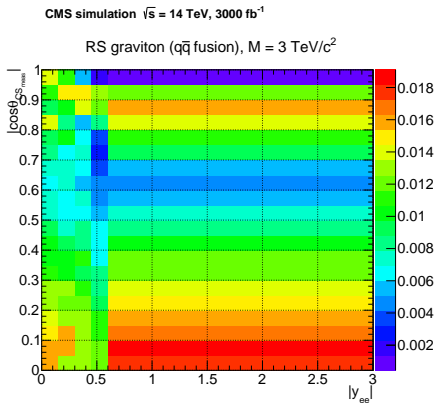
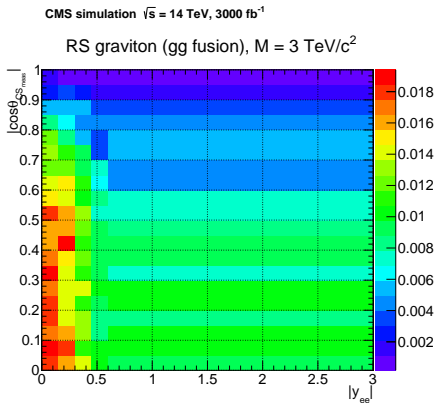
2D

| | 100 fb ⁻¹ (13 TeV) | 300 fb ⁻¹ (14 TeV) | 3000 fb ⁻¹ (14 TeV) |
|---------------------------------------------|----------------------------------------|----------------------------------------|----------------------------------------|
| R-S graviton (M = 3 TeV/c ²) 2D | 0.37 ^{+0.31} _{-0.30} | 0.36 ^{+0.13} _{-0.13} | 0.37 ^{+0.05} _{-0.04} |
| R-S graviton (M = 4 TeV/c ²) 2D | 0.34 ^{+0.66} _{-0.34} | 0.20 ^{+0.45} _{-0.20} | 0.24 ^{+0.13} _{-0.15} |

Predicted values

| | |
|-----------------------|------|
| RS graviton M = 3 TeV | 0.38 |
| RS graviton M = 4 TeV | 0.25 |

gg fraction measurement: templates 2D



N.B. The drop at $|\cos\theta_{CS}| \approx 0.6$ and $|y_{ee}| > 0.6$ in the right distribution is an acceptance effect (one of the electrons often in the gap).

- The increase of the LHC beams energy in 2015 will strongly enhance the production cross sections of TeV particles
- The dielectron decay mode is a clean channel where a discovery could be made in the first months of the data taking.
- In such a case, the measurement of three properties were investigated: spin, A_{FB} , production mode.
- The expected separation and measurement uncertainties were computed for different scenarios covering the mass range to which the next LHC runs will be sensitive.
- The performances of a 1d method (based on $\cos\theta_{CS}$) were compared to a 2d method (based on $\cos\theta_{CS}$, $|y_{ee}|$).
- The second method leads to slightly better results although being more model dependent.
- **Precision strongly improved from $300 \text{ fb}^{-1} \rightarrow$ to 3000 fb^{-1}**

Stay tuned !

$$\begin{aligned}
& \kappa * p_{A_{FB}=-1} + (1 - \kappa) * p_{A_{FB}=+1} \\
\propto & \kappa(1 + \cos^2 \theta + 2 \cos \theta) + (1 - \kappa)(1 + \cos^2 \theta + 2 \cos \theta) \\
\propto & 1 + \cos^2 \theta + (4\kappa - 2) \cos \theta \\
\propto & 1 + \cos^2 \theta + \frac{8}{3} A_{FB} \cos \theta
\end{aligned}$$

Where the last equation comes from the fact that:

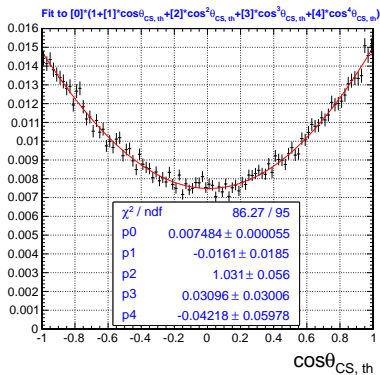
$$\begin{aligned}
\sigma_F &= K \times \int_0^{2\pi} d\phi \int_0^1 d \cos \theta (1 + \cos^2 \theta + \frac{8}{3} A_{FB} \cos \theta) = 2\pi K (\frac{4}{3} + \frac{4}{3} A_{FB}) \\
\sigma_B &= K \times \int_0^{2\pi} d\phi \int_{-1}^0 d \cos \theta (1 + \cos^2 \theta + \frac{8}{3} A_{FB} \cos \theta) = 2\pi K (\frac{4}{3} - \frac{4}{3} A_{FB})
\end{aligned}$$

Hence

$$\frac{\sigma_F - \sigma_B}{\sigma_F + \sigma_B} = A_{FB}$$

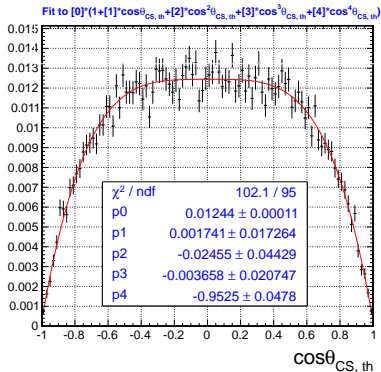
Therefore:

$$A_{FB} = \frac{3}{4}(2\kappa - 1)$$

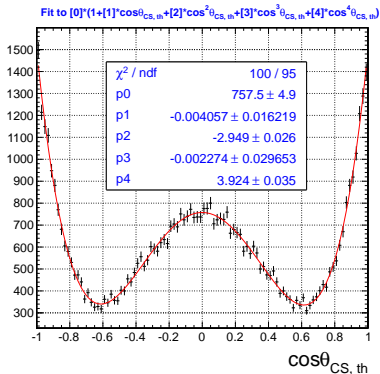
$Z'_\Psi, M = 3 \text{ TeV}/c^2$ 

RS graviton: $\cos\theta_{CS,th}$ distributions for gg vs $q\bar{q}$

RS graviton (gg fusion), $M = 3 \text{ TeV}/c^2$

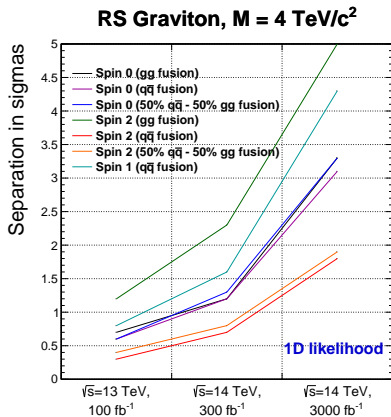
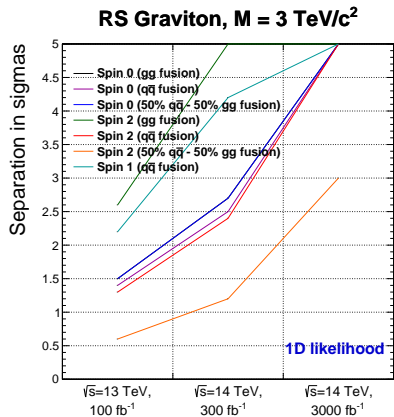


RS graviton ($q\bar{q}$ fusion), $M = 3 \text{ TeV}/c^2$

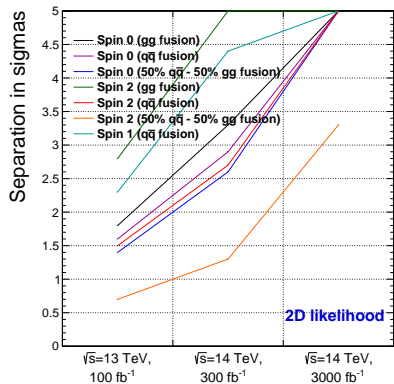


Left: $\propto 1 - \cos^4 \theta_{CS,th}$

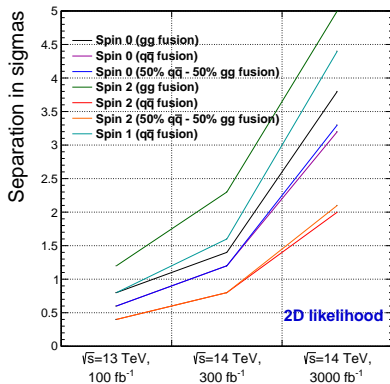
Right: $\propto 1 - 3 \cos^2 \theta_{CS,th} + 4 \cos^4 \theta_{CS,th}$



RS Graviton, $M = 3 \text{ TeV}/c^2$



RS Graviton, $M = 4 \text{ TeV}/c^2$



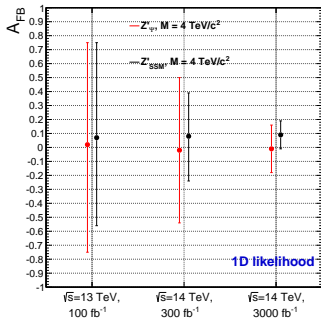
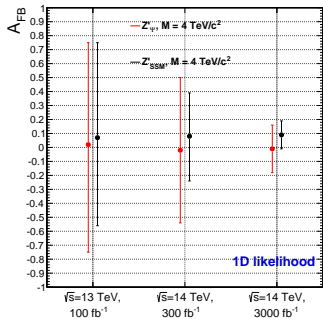
Spin Measurement: Results 1D

| | 100 fb^{-1} (13 TeV) | 300 fb^{-1} (14 TeV) | 3000 fb^{-1} (14 TeV) |
|------------------------------------------|--------------------------------|--------------------------------|---------------------------------|
| RS grav (3 TeV) vs Spin 0 (gg), 1D | 1.5 | 2.7 | > 5 |
| RS grav (3 TeV) vs Spin 0 (qqbar), 1D | 1.4 | 2.5 | > 5 |
| RS grav (3 TeV) vs Spin 0 (qqbar-gg), 1D | 1.5 | 2.7 | > 5 |
| RS grav (3 TeV) vs Spin 2 (gg), 1D | 2.6 | > 5 | > 5 |
| RS grav (3 TeV) vs Spin 2 (qqbar), 1D | 1.3 | 2.4 | > 5 |
| RS grav (3 TeV) vs Spin 2 (qqbar-gg), 1D | 0.6 | 1.2 | 3 |
| RS grav (3 TeV) vs Spin 1 (qqbar), 1D | 2.2 | 4.2 | > 5 |
| RS grav (4 TeV) vs Spin 0 (gg), 1D | 0.7 | 1.2 | 3.3 |
| RS grav (4 TeV) vs Spin 0 (qqbar), 1D | 0.6 | 1.2 | 3.1 |
| RS grav (4 TeV) vs Spin 0 (qqbar-gg), 1D | 0.6 | 1.3 | 3.3 |
| RS grav (4 TeV) vs Spin 2 (gg), 1D | 1.2 | 2.3 | > 5 |
| RS grav (4 TeV) vs Spin 2 (qqbar), 1D | 0.3 | 0.7 | 1.8 |
| RS grav (4 TeV) vs Spin 2 (qqbar-gg), 1D | 0.4 | 0.8 | 1.9 |
| RS grav (4 TeV) vs Spin 1 (qqbar), 1D | 0.8 | 1.6 | 4.3 |
| Z' Psi (3 TeV) vs Spin 0 (gg), 1D | 1.3 | 2.3 | > 5 |
| Z' Psi (3 TeV) vs Spin 0 (qqbar), 1D | 1.3 | 2.3 | > 5 |
| Z' Psi (3 TeV) vs Spin 0 (qqbar-gg), 1D | 1.3 | 2.3 | > 5 |
| Z' Psi (3 TeV) vs Spin 2 (gg), 1D | 2.9 | > 5 | > 5 |
| Z' Psi (3 TeV) vs Spin 2 (qqbar), 1D | 2.2 | 4.1 | > 5 |
| Z' Psi (3 TeV) vs Spin 2 (qqbar-gg), 1D | 1.9 | 3.5 | > 5 |
| Z' Psi (4 TeV) vs Spin 0 (gg), 1D | 0.4 | 0.8 | 2.1 |
| Z' Psi (4 TeV) vs Spin 0 (qqbar), 1D | 0.5 | 1.0 | 2.6 |
| Z' Psi (4 TeV) vs Spin 0 (qqbar-gg), 1D | 0.5 | 0.9 | 2.3 |
| Z' Psi (4 TeV) vs Spin 2 (gg), 1D | 1.1 | 2.1 | > 5 |
| Z' Psi (4 TeV) vs Spin 2 (qqbar), 1D | 0.8 | 1.6 | 4.5 |
| Z' Psi (4 TeV) vs Spin 2 (qqbar-gg), 1D | 0.7 | 1.4 | 3.7 |

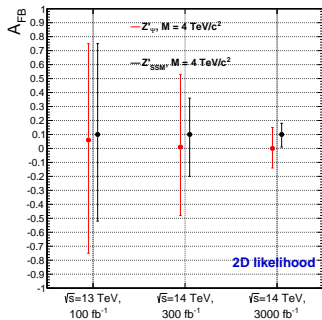
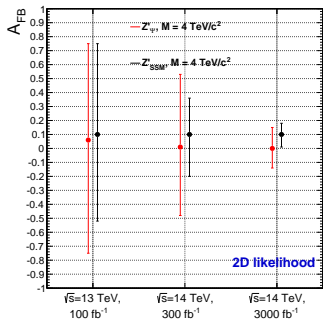
Spin Measurement: Results 2D

| | 100 fb ⁻¹ (13 TeV) | 300 fb ⁻¹ (14 TeV) | 3000 fb ⁻¹ (14 TeV) |
|------------------------------------------|-------------------------------|-------------------------------|--------------------------------|
| RS grav (3 TeV) vs Spin 0 (gg), 2D | 1.8 | 3.3 | > 5 |
| RS grav (3 TeV) vs Spin 0 (qqbar), 2D | 1.6 | 2.9 | > 5 |
| RS grav (3 TeV) vs Spin 0 (qqbar-gg), 2D | 1.4 | 2.6 | > 5 |
| RS grav (3 TeV) vs Spin 2 (gg), 2D | 2.8 | > 5 | > 5 |
| RS grav (3 TeV) vs Spin 2 (qqbar), 2D | 1.5 | 2.7 | > 5 |
| RS grav (3 TeV) vs Spin 2 (qqbar-gg), 2D | 0.7 | 1.3 | 3.3 |
| RS grav (3 TeV) vs Spin 1 (qqbar), 2D | 2.3 | 4.4 | > 5 |
| RS grav (4 TeV) vs Spin 0 (gg), 2D | 0.8 | 1.4 | 3.8 |
| RS grav (4 TeV) vs Spin 0 (qqbar), 2D | 0.6 | 1.2 | 3.2 |
| RS grav (4 TeV) vs Spin 0 (qqbar-gg), 2D | 0.6 | 1.2 | 3.3 |
| RS grav (4 TeV) vs Spin 2 (gg), 2D | 1.2 | 2.3 | > 5 |
| RS grav (4 TeV) vs Spin 2 (qqbar), 2D | 0.4 | 0.8 | 2 |
| RS grav (4 TeV) vs Spin 2 (qqbar-gg), 2D | 0.4 | 0.8 | 2.1 |
| RS grav (4 TeV) vs Spin 1 (qqbar), 2D | 0.8 | 1.6 | 4.4 |
| Z' Psi (3 TeV) vs Spin 0 (gg), 2D | 1.9 | 3.5 | > 5 |
| Z' Psi (3 TeV) vs Spin 0 (qqbar), 2D | 1.3 | 2.3 | > 5 |
| Z' Psi (3 TeV) vs Spin 0 (qqbar-gg), 2D | 1.5 | 2.6 | > 5 |
| Z' Psi (3 TeV) vs Spin 2 (gg), 2D | 3.1 | > 5 | > 5 |
| Z' Psi (3 TeV) vs Spin 2 (qqbar), 2D | 2.2 | 4.1 | > 5 |
| Z' Psi (3 TeV) vs Spin 2 (qqbar-gg), 2D | 2 | 3.8 | > 5 |
| Z' Psi (4 TeV) vs Spin 0 (gg), 2D | 0.7 | 1.3 | 3.4 |
| Z' Psi (4 TeV) vs Spin 0 (qqbar), 2D | 0.5 | 1.0 | 2.6 |
| Z' Psi (4 TeV) vs Spin 0 (qqbar-gg), 2D | 0.5 | 1.0 | 2.6 |
| Z' Psi (4 TeV) vs Spin 2 (gg), 2D | 1.2 | 2.3 | > 5 |
| Z' Psi (4 TeV) vs Spin 2 (qqbar), 2D | 0.8 | 1.6 | 4.4 |
| Z' Psi (4 TeV) vs Spin 2 (qqbar-gg), 2D | 0.8 | 1.5 | 3.9 |

A_{FB} measurement, $M=4$ TeV: Results 1D



A_{FB} measurement, $M=4$ TeV: Results 2D



| | 100 fb ⁻¹ (13 TeV) | 300 fb ⁻¹ (14 TeV) | 3000 fb ⁻¹ (14 TeV) |
|-------------------------------------------|-----------------------------------------|-----------------------------------------|-----------------------------------------|
| Z'_ψ (M = 3 TeV/c ²) 1D | -0.01 ^{+0.39} _{-0.36} | 0.00 ^{+0.18} _{-0.19} | -0.01 ^{+0.06} _{-0.06} |
| Z'_{SSM} (M = 3 TeV/c ²) 1D | 0.07 ^{+0.21} _{-0.22} | 0.07 ^{+0.11} _{-0.10} | 0.07 ^{+0.04} _{-0.03} |
| Z'_ψ (M = 4 TeV/c ²) 1D | 0.02 ^{+0.73} _{-0.77} | -0.02 ^{+0.52} _{-0.52} | -0.01 ^{+0.17} _{-0.17} |
| Z'_{SSM} (M = 4 TeV/c ²) 1D | 0.07 ^{+0.68} _{-0.63} | 0.08 ^{+0.31} _{-0.32} | 0.09 ^{+0.10} _{-0.10} |

Drell-Yan (1056 evts, M > 3 TeV/c²) 1D 0.59^{+0.06}_{-0.06}

| | 100 fb ⁻¹ (13 TeV) | 300 fb ⁻¹ (14 TeV) | 3000 fb ⁻¹ (14 TeV) |
|-------------------------------------------|----------------------------------------|----------------------------------------|-----------------------------------------|
| Z'_ψ (M = 3 TeV/c ²) 2D | 0.01 ^{+0.31} _{-0.35} | 0.00 ^{+0.16} _{-0.16} | -0.01 ^{+0.05} _{-0.05} |
| Z'_{SSM} (M = 3 TeV/c ²) 2D | 0.09 ^{+0.19} _{-0.20} | 0.07 ^{+0.10} _{-0.10} | 0.08 ^{+0.03} _{-0.03} |
| Z'_ψ (M = 4 TeV/c ²) 2D | 0.06 ^{+0.69} _{-0.81} | 0.01 ^{+0.52} _{-0.49} | -0.00 ^{+0.15} _{-0.14} |
| Z'_{SSM} (M = 4 TeV/c ²) 2D | 0.10 ^{+0.65} _{-0.62} | 0.10 ^{+0.26} _{-0.30} | 0.10 ^{+0.08} _{-0.09} |

Drell-Yan (1056 evts, M > 3 TeV/c²) 2D 0.62^{+0.04}_{-0.04}

Predicted values

| | up quarks | down quarks | $\sqrt{s} = 13$ TeV pp collisions |
|---------------------|---------------|-------------|-----------------------------------|
| Z'_ψ | 0 | 0 | 0 |
| Z'_1 | (no coupling) | -0.75 | -0.75 |
| Z'_{SSM} | 0.075 | 0.105 | 0.08 |
| Drell-Yan M > 3 TeV | 0.595 | 0.625 | 0.60 |

Differences between median and predicted values (≈ 0.01) due to limited statistics used to build the pdf for generation and likelihood and to limited nb of PE generated (1000).

$$\cos \theta_{CS_{meas}} = \frac{p_{z,\bar{l}}}{|p_{z,\bar{l}}|} 2 \frac{E_l \cdot p_{z,\bar{l}} - E_{\bar{l}} \cdot p_{z,l}}{M_{\bar{l}\bar{l}} \sqrt{M_{\bar{l}\bar{l}}^2 + P_{T,\bar{l}}^2}}$$

